JOURNAL OF CATALYSIS 135, 467–480 (1992)

Kinetic Studies of the Oxidative Coupling of Methane over a NaOH/CaO Catalyst

L. LEHMANN AND M. BAERNS[1]

Chemical Technology and Reaction Engineering, Ruhr-University Bochum, P.O. Box 102148, D-4630 Bochum 1, Germany

Received October 23, 1990; revised August 8, 1991

The effects of the partial pressures of oxygen and methane as well as temperature on the rates of C_2 hydrocarbon formation, carbon oxide formation, and total methane conversion in the oxidative coupling of methane over a NaOH/CaO catalyst were studied at differential operating conditions in a microcatalytic fixed-bed reactor. Temperature and partial pressures of the reactants were varied within the following ranges: 933 K $\leq T \leq$ 1033 K, 5 kPa $\leq P^{\circ}_{CH_4} \leq$ 80 kPa, 0.3 kPa $\leq P^{\circ}_{O_2} \leq$ 20 kPa. The rate of CO_X formation was of 0.5 order in methane as well as in oxygen; the rate of C_2 hydrocarbon formation was first order in methane while it passed through a maximum with respect to oxygen partial pressure. The rate of methane conversion was well described by a power-law rate equation. Mechanistic assumptions derived from these kinetic results and corroborated by kinetic isotope effects are presented. In addition, kinetic equations for C_2 hydrocarbon formation, carbon oxide formation, and methane conversion as reported in the literature were scrutinized for their applicability to describing the experimental data obtained in this work.

INTRODUCTION

The kinetics of the oxidative coupling reaction of methane to C_{2+} hydrocarbons have been studied by various authors on the basis of different reaction schemes (*1–33*). As can be derived from their results, no complete agreement on the dependence of the various reaction steps on the partial pressures of the reactants exists even when similar catalysts are considered.

Against this background the effects of the partial pressures of methane and oxygen on the rates of the primary reaction steps leading to ethane plus ethylene and to CO_X were studied over a wide range of reactant partial pressures (5 kPa $\leq P^{\circ}_{CH_4} \leq$ 80 kPa, 0.3 kPa $\leq P^{\circ}_{O_2} \leq$ 20 kPa) and temperatures (933 K $\leq T \leq$ 1033 K) applying a NaOH/CaO catalyst. Power-law equations but also Langmuir–Hinshelwood-type rate equations were used for describing the kinetic data. Accounting for the kinetic relationships, mechanistic assumptions are presented and discussed in relation to kinetic isotope effects observed in another study (*34*). In addition to the equations applied in this work, kinetic equations proposed by other researchers were also tested for applicability to the experimental data obtained in this work.

METHODS

The rates of C_2 hydrocarbon and carbon oxide formation were measured at nearly differential operating conditions; i.e., oxygen conversion was always less than 20% and methane conversion was usually below 2%.

Apart from the fact that reaction rates can be easily approximated by this method, the differential reactor was chosen mainly for two reasons:

(1) Consecutive reactions of C_2 hydrocarbons to CO_X are negligible. The total oxidation of ethane and ethylene was investigated over the NaOH/CaO catalyst in another work (*35*); at differential conversion grades

[1] To whom correspondence should be addressed.

0021-9517/92 $5.00

the conversion rate of C_2 hydrocarbons is slow (at the maximum 1.5%) compared to their formation rate.

(2) Preliminary experiments carried out by the present authors demonstrated the inhibiting effect of carbon dioxide on the formation of carbon oxides as well as on that of hydrocarbons. This is in agreement with the results of Campbell and Lunsford (*36*), who demonstrated the detrimental effect of carbon dioxide on the rate of methyl radical formation over a Na/CaO catalyst. Since only low concentrations of CO_2 resulted from the differential conversion grades, its inhibitory effect on the reaction rates was neglected as a first approximation.

For the reasons outlined above, a parallel-path reaction scheme seemed justified as a basis for the kinetic evaluation:

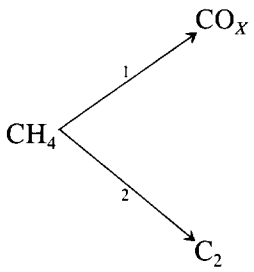

(1)

Ethane and ethylene were lumped as a pseudo-compound, since a significant amount of C_2H_6 is consumed by gas-phase oxidative and thermal dehydrogenation leading to C_2H_4 (catalytic reactions may also occur).

Blank runs confirmed that homogeneous methane oxidation could be neglected compared to the catalytic route. Rate limitation by external or internal mass transfer was proven to be negligible by applying suitable criteria.

EXPERIMENTAL

Catalyst

The NaOH/CaO catalyst was prepared by impregnating $Ca(OH)_2$ particles (d_p = 0.16 – 0.36 mm) with an aqueous 2.1 *M* NaOH solution by the incipient wetness method; the loading amounted to 11 mol% NaOH. The catalyst precursor was dried at 400 K and subsequently pressed to pellets (h_p = 4 mm, d_p = 4 mm) at 60 bar. The pellets were then calcined at 1073 K in air whereby $Ca(OH)_2$ was transformed into CaO. Smaller-sized catalyst fractions were obtained by crushing the pellets; the grain size of the catalyst fraction applied for the kinetic measurements amounted to 100–160 μm.

Apparatus

A quartz-made tubular catalytic fixed-bed reactor with an internal diameter of 6 mm was used for the kinetic measurements. After the catalyst layer the internal diameter was reduced to 2 mm in order to minimize the post-catalytic residence time, thereby reducing any consecutive total oxidation. The catalyst particles were diluted with quartz granules of the same size in order to avoid severe temperature gradients within the catalytic bed. The temperature within the catalyst layer was measured by an axially movable thermocouple placed in a thin quartz tube (outer diameter, 2.5 mm); a maximum temperature gradient of 4 K over the catalyst layer was observed. The reactor effluent was analyzed on-line by gas chromatography: H_2, O_2, N_2, CO, CH_4, and CO_2 were separated and analyzed by a Carbosieve SII column connected to a thermal conductivity detector. Ethylene, ethane, propylene, propane, and C_4 hydrocarbons were separated and analyzed by a Porapak Q column linked to a flame ionization detector; however, no measurable amounts of C_3 and higher hydrocarbons were observed.

Experimental Conditions

Kinetics were measured at a constant catalyst activity at atmospheric pressure in the temperature range between 933 and 1033 K in intervals of 20 K. The initial partial pressure of oxygen was varied (0.3–20 kPa) at a constant initial pressure of methane (70 kPa) and the initial partial pressure of methane was varied (5–80 kPa) while keeping the ini-

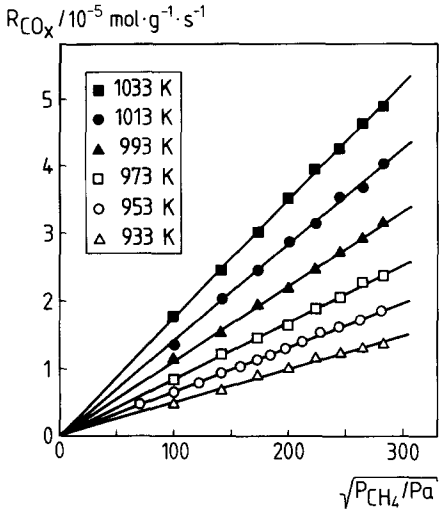

FIG. 1. Rate of carbon oxide formation versus the square root of methane partial pressure at various temperatures ($P^{\circ}_{O_2}$ = 7.5 kPa).

tial pressure of oxygen (7.5 kPa) constant; the balance to 100 kPa was always nitrogen.

RESULTS

In the following section, results on the kinetics and on the kinetic isotope effects for carbon oxide and C_2 hydrocarbon formation are presented.

Rate of Carbon Oxide Formation

The rate of carbon oxide formation depends both on methane and oxygen partial pressure with a reaction order of 0.5:

$$R_{CO_X} = k_1 \cdot P^{0.5}_{CH_4} \cdot P^{0.5}_{O_2} \qquad (2a)$$

with

$$k_1 = k_{1.0} \cdot \exp(-E_a/RT). \qquad (2b)$$

This kinetic relationship is illustrated in Figs. 1 and 2, in which the rates of carbon oxide formation are plotted versus the square roots of methane and of oxygen partial pressure. A similar kinetic relationship has been reported by McCarty *et al.* (*18*) for a Na-promoted CaO catalyst (similar to the catalyst used in the present work) at 1000 K: the order in methane was 0.5 ± 0.2 and in oxygen 0.6 ± 0.1. The same kinetic equation was found by Lo *et al.* (*16*) for a K–Sb/SiO_2 catalyst; apparent reaction orders of methane and oxygen for carbon oxide formation that are close to 0.5 have also been reported by Miro *et al.* (*30*) for a Li/$NiTiO_3$ catalyst.

The frequency factor and the activation energy for carbon oxide formation derived from an Arrhenius plot (no figure shown) are $(2.77 \pm 1.03) \times 10^{-4}$ mol·g^{-1}·s^{-1}·Pa^{-1} and 101 ± 3 kJ/mol.

Rate of C_2 Hydrocarbon Formation

The rate of hydrocarbon formation is first order in methane partial pressure over the whole temperature range studied, as can easily be seen in Fig. 3 in which the rate of hydrocarbon formation is plotted versus the methane partial pressure:

$$R_{C_2} \sim P^1_{CH_4} \qquad (3)$$

The same kinetic relationship has been observed by McCarty *et al.* (*18*) and by Lo *et al.* (*16*) for the above-mentioned catalysts. Furthermore, apparent reaction orders in methane for hydrocarbon formation close to 1 have been reported by Miro *et al.* (*30*) for Li/$NiTiO_3$ as catalyst.

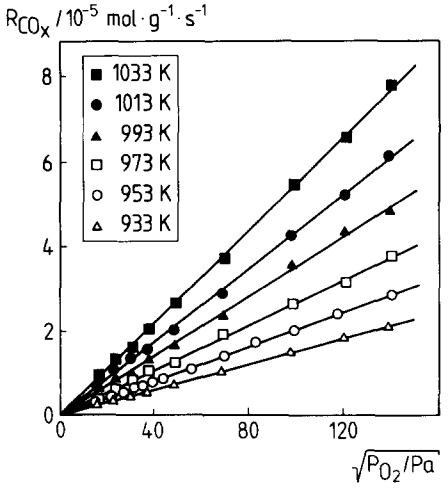

FIG. 2. Rate of carbon oxide formation versus the square root of oxygen partial pressure at various temperatures ($P^{\circ}_{CH_4}$ = 70 kPa).

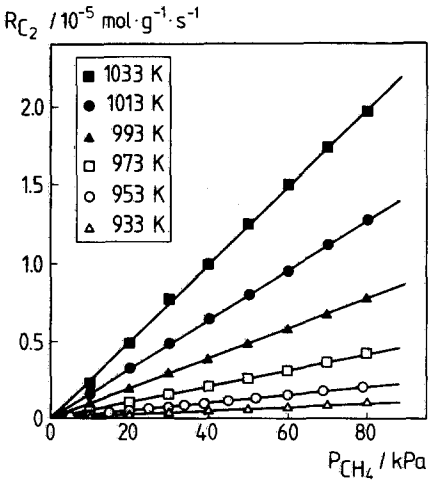

FIG. 3. Rate of hydrocarbon formation versus methane partial pressure at various temperatures ($P^{\circ}_{O_2}$ = 7.5 kPa).

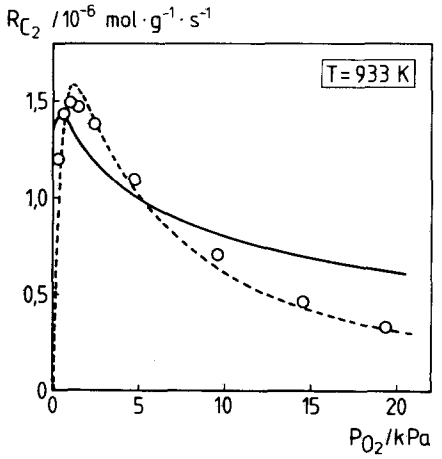

FIG. 5. Rate of hydrocarbon formation versus oxygen partial pressure at 933 K ($P^{\circ}_{CH_4}$ = 70 kPa). Symbols, experimental data. (—) Data calculated according to model 1 (Eq. (9)). (---) Data calculated according to model 2 (Eq. (10)).

With respect to oxygen partial pressure, the hydrocarbon formation rate passes through a maximum (see Figs. 4, 5, and 6). With increasing temperature this maximum is shifted to higher oxygen partial pressures and the inhibiting effect leading to a rate decrease is diminished. The relation between R_{C_2} and P_{O_2} as obtained in this study, i.e., a rate increase with oxygen partial pressure in its low concentration range and a decrease at high oxygen concentrations, consolidates earlier results that appeared to be different. Otsuka and Jinno (6) reported that the hydrocarbon formation rate passes

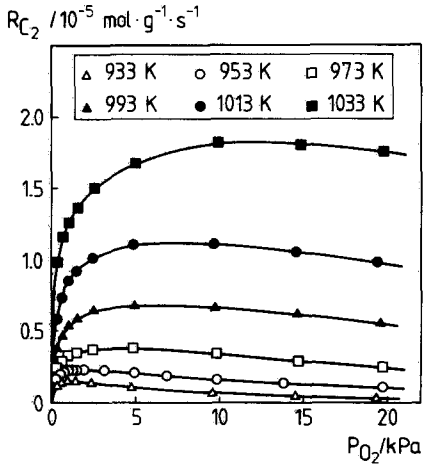

FIG. 4. Rate of hydrocarbon formation versus oxygen partial pressure at various temperatures ($P^{\circ}_{CH_4}$ = 70 kPa).

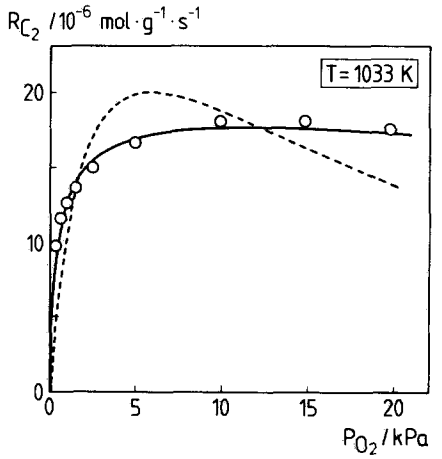

FIG. 6. Rate of hydrocarbon formation versus oxygen partial pressure at T = 1033 K (P_{CH_4} = 70 kPa). Symbols, experimental data. (—) Data calculated according to model 1 (Eq. (9)). (---) Data calculated according to model 2 (Eq. (10)).

through a maximum in dependence on the oxygen partial pressure over a Sm_2O_3 catalyst between 873 and 973 K. Tagawa and Imai (*11*) found negative reaction orders when applying CH_4/O_2 ratios below 4 and positive reaction orders for CH_4/O_2 ratios above 4 using a $LaAlO_3$ catalyst at 983 K. Hatano and Otsuka (*17*) observed a negative dependence of the hydrocarbon formation rate on the oxygen partial pressure over a $LiNiO_2$ catalyst between 953 and 973 K at oxygen partial pressures higher than 1 kPa. Furthermore, McCarty *et al.* (*18*) observed a reaction order of -0.5 at oxygen partial pressures between 10 and 50 kPa for the sodium-promoted CaO catalyst at 1000 K, while Iwamatsu and Aika (*27*) reported a positive reaction order for a catalyst between 973 and 1023 K at oxygen partial pressures below 3 kPa. For hydrocarbon formation over a $Na/NiTiO_3$ catalyst, Miro *et al.* (*30*) found a negative reaction order with respect to oxygen (-0.3) at 973 K and orders of 0.1 and 0.4 at 1023 and 1073 K, respectively. Finally, the same maximum-type behavior as that observed in this work has been reported by Lunsford and coworkers for a Li/MgO catalyst at 893 K (*2*) and for a Na/CaO catalyst at 898 K (*15*).

The temperature dependence of the hydrocarbon formation rate was considered at a low oxygen partial pressure of 0.3 kPa, i.e., in the range of a positive reaction order in oxygen and at a high partial pressure of 20 kPa, where the respective reaction order is negative. The apparent activation energy for hydrocarbon formation derived from an Arrhenius-type evaluation amounts to 167 kJ/mol at $P_{O_2} = 0.3$ kPa and 317 kJ/mol at $P_{O_2} = 20$ kPa (no figure shown); it increases with increasing oxygen partial pressure, because at high oxygen pressures the inverse temperature dependence of the inhibition has a stronger influence on the overall temperature dependence. In both cases the apparent activation energy is significantly higher than that for carbon oxide formation, which is 101 kJ/mol.

Rate of Methane Conversion

For each temperature applied, the rate of methane conversion was fitted to a power-law rate equation for determining k_3, m, and n:

$$-R_{CH_4} = k_3 \cdot P_{CH_4}^m \cdot P_{O_2}^n \qquad (4)$$

The kinetic parameters obtained are listed in Table 1. Furthermore, the methane conversion rate was fitted to an overall power-law rate equation covering all temperatures by introducing $k_3 = k_{3,0} \cdot \exp(-E/RT)$ into Eq. 4; the results are given in the last row of Table 1. The activation energy amounted to 137 ± 4 kJ/mol.

Kinetic Isotope Effects

As a basis for further discussion of the kinetic results described above, reference is made to experimentally observed kinetic isotope effects for the formation of carbon oxides and C_2 hydrocarbons, which are reported elsewhere in more detail (*34*). When CH_4 was substituted by CD_4, the carbon oxide formation rate remained constant within experimental accuracy, whereas the rate of hydrocarbon formation decreased significantly (see Table 2).

DISCUSSION

In the following, some mechanistic conclusions derived from the kinetic results are discussed.

Reaction Scheme

The formation of methyl radicals has often been proposed to be the rate-determining step in the oxidative coupling reaction of methane. It is often assumed that these methyl radicals are released into the gas phase, where they either recombine to ethane or react further with oxygen-containing species to form carbon oxides. If this reaction scheme were valid and the rate-determining step were the methyl radical formation in both competitive reaction steps, the same kinetic isotope effects would be expected for carbon oxide and hydrocar-

TABLE 1

Kinetic Parameters for the Methane Conversion Rate According to Eq. (4)

T (K)	k_3[a]	m	n
933	$(1.32 \pm 0.28) \cdot 10^{-9}$	0.56 ± 0.02	0.35 ± 0.01
953	$(1.51 \pm 0.14) \cdot 10^{-9}$	0.58 ± 0.02	0.35 ± 0.01
973	$(1.53 \pm 0.30) \cdot 10^{-9}$	0.61 ± 0.02	0.35 ± 0.01
993	$(1.64 \pm 0.27) \cdot 10^{-9}$	0.64 ± 0.02	0.34 ± 0.01
1013	$(2.42 \pm 0.31) \cdot 10^{-9}$	0.65 ± 0.02	0.32 ± 0.01
1033	$(2.46 \pm 0.28) \cdot 10^{-9}$	0.68 ± 0.02	0.32 ± 0.01

T (K)	$k_{3,0}$[a]	E_a (kJ · mol^{-1})	m	n
933–1033	$(2.46 \pm 0.77) \times 10^{-2}$	137 ± 4	0.65 ± 0.05	0.33 ± 0.03

[a] Units of mol · g^{-1} · s^{-1} · Pa^{-m-n}.

bon formation. Since this is not the case (see Table 2 and also (*37–40*)), C_2 and CO_X are assumed to be formed by separate reaction pathways involving different rate-determining steps and different intermediates, as proposed earlier by Nelson *et al.* (*37*) and Mirodatos *et al.* (*39*). Therefore, the mechanism for carbon oxide formation and for hydrocarbon formation is treated separately in the following.

Carbon Oxide Formation

The carbon oxide formation is of 0.5 order in methane as well as in oxygen. This kinetic relationship suggests that methane and oxygen reacting to CO_X are adsorbed dissociatively in fast reaction steps on the catalyst surface. The slow and rate-determining step for CO_X formation is then assumed to be the reaction between a CH_3 species and an O species reacting via various intermediates to the carbon oxides:

$$CH_3(ads) + O(ads) \xrightarrow{k_1} CH_3O(ads) \rightarrow \rightarrow \rightarrow CO_X \quad (5)$$

Since no C–H bond is broken in this reaction step, no kinetic isotope effect should be observed, which in fact agrees with experimental evidence (see Table 2). It should be noted that considering solely the kinetics, no conclusions can be drawn concerning the nature of the CH_3 and O species.

TABLE 2

Primary Kinetic Isotope Effects for Carbon Oxide and Hydrocarbon Formation over a NaOH/CaO Catalyst

T (K)	k_H/k_D	
	R_{CO_X}	R_{C_2}
933	0.99 ± 0.06	2.18 ± 0.13
973	1.04 ± 0.06	1.91 ± 0.10
1013	1.02 ± 0.05	1.60 ± 0.09

Hydrocarbon Formation

The kinetic results for hydrocarbon formation and the mechanistic assumptions derived therefrom are summarized below.

(1) The hydrocarbon formation rate passes through a maximum with respect to oxygen partial pressure. With increasing temperature this maximum is shifted to higher oxygen partial pressures and the inhibiting effect is reduced. From this behavior it is concluded that the inhibitory effect is due to adsorption of oxygen on the catalyst surface; the effect is reduced by increasing the temperature and decreasing the partial pressure due to lesser adsorption. This conclusion is in agreement with Hatano and Otsuka (*17*), who ascribed the inhibiting effect

of oxygen on C_2 hydrocarbon formation over $LiNiO_2$ to competitive adsorption of methane and oxygen on the active sites for hydrocarbon formation. The occurrence of a rate maximum cannot be explained by total oxidation of ethane and ethylene, since these consecutive reactions were proven to be negligible at the experimental conditions applied in this work. Lin *et al.* (*15*) explained the occurrence of a maximum in hydrocarbon formation and methane conversion with respect to oxygen partial pressure by a gas-phase free radical chain mechanism involving the equilibrium reaction of methyl radicals with oxygen:

$$CH_3\cdot + O_2 \rightleftharpoons CH_3O_2\cdot \qquad (6)$$

This reaction has often been used as an explanation for the influence of oxygen partial pressure and temperature on the hydrocarbon selectivity over nearly all catalysts, since with increasing temperature and decreasing oxygen pressure the equilibrium is shifted to the left side (*41*). However, the proposed radical mechanism implies that carbon oxides and hydrocarbons are formed via the same intermediate that was excluded due to different kinetic isotope effects. Furthermore, by a sensitivity analysis of radical reactions during oxidative methane coupling in the gas phase, reaction (6) is shown to be of minor importance (*42*). This is in agreement with Lunsford (*43*), who observed that modeling results are essentially the same when reaction (6) is omitted. It should be mentioned at this point that in Lunsford's opinion the role of $CH_3O_2\cdot$ in equilibrium with $CH_3\cdot$ and O_2 appears to be less significant than previously thought (*43*). Hence, the influence of temperature and oxygen partial pressure on equilibrium reaction (6) can be dismissed as an explanation for the inhibiting effect of oxygen on hydrocarbon formation.

(2) CH_4 and O_2 involved in hydrocarbon formation are adsorbed on the same sites. If methane were adsorbed on a different site or reacted from the gas phase according to an Eley–Rideal mechanism an inhibitory effect of oxygen could not be observed but the rate of hydrocarbon formation would approach asymptotically a constant value with increasing oxygen partial pressure.

(3) The hydrocarbon formation is first order in methane. This relationship suggests that methane involved in hydrocarbon formation is only weakly adsorbed in molecular form so that the surface coverage of methane is very low and any inhibition by adsorbed methane can be neglected.

(4) It is generally accepted that ethane formation occurs via the recombination of two methyl radicals.

(5) The rate-determining step for hydrocarbon formation involves C–H bond rupture, since a kinetic isotope effect for hydrocarbon formation has been observed in this work (see Table 2) and also by various other authors (*37–40, 44, 45*). As mentioned by Cant *et al.* (*46*), another possibility for the rate-determining step over a Li/MgO catalyst is the breaking of an O–H bond during rearrangement of $[Li^+OH^-]$ sites. However, this reaction step was proven by Cant and co-workers to not be rate determining since the conversion rate of methane with D_2O addition was equal to the rate of methane conversion with H_2O addition. According to Burch *et al.* (*31*), the rate-determining step over a $Na/MnO_X/SiO_X$ catalyst is the reduction of an active centre on a reducible metal oxide surface by methane. This proposal cannot be transferred to the NaOH/CaO catalyst investigated in this work, since this system is not reducible.

Taking items 1 to 5 into consideration, the rate-determining step for hydrocarbon formation is proposed to be the formation of methyl radicals by reaction of weakly adsorbed molecular methane with either dissociatively or molecularly adsorbed oxygen involving C–H bond rupture:

$$CH_4(\text{ads}) + O_X(\text{ads}) \xrightarrow{k_2} CH_3\cdot(\text{ads}) + HO_X\cdot(\text{ads}) \qquad (7)$$

$x = 1$: dissociative adsorption of oxygen

$x = 2$: molecular adsorption of oxygen.

TABLE 3

Kinetic Parameters for Model 1 (Eq. (9)) and Model 2 (Eq. (10))

T (K)	$k_{2,1}$[a]	$k_{2,2}$[a]	$b_{2,1}$[b]	$b_{2,2}$[b]
933	0.82 ± 0.07	0.93 ± 0.03	26.6 ± 12.3	9.38 ± 0.86
953	1.25 ± 0.03	1.47 ± 0.06	8.56 ± 1.45	5.37 ± 0.56
973	2.04 ± 0.05	2.52 ± 0.17	3.57 ± 0.53	3.36 ± 0.51
993	3.75 ± 0.05	4.57 ± 0.31	1.80 ± 0.16	2.49 ± 0.38
1013	6.23 ± 0.05	7.52 ± 0.56	1.48 ± 0.08	2.30 ± 0.39
1033	10.2 ± 0.20	11.9 ± 1.04	0.99 ± 0.11	1.86 ± 0.38

[a] Units of 10^{-10} mol · g^{-1} · s^{-1}.
[b] Units of 10^{-4} Pa.

According to Eq. (7) the hydrocarbon formation is proportional to the coverage of methane and oxygen on the catalyst surface:

$$R_{C_2} = k_2 \cdot \theta_{CH_4} \cdot \theta_{O_X}. \tag{8}$$

Assuming Langmuir–Hinshelwood adsorption the following kinetic equations can be derived.

Model 1. Oxygen involved in hydrocarbon formation is dissocatively adsorbed ($x = 1$)

$$R_{C_2} = \frac{k_{2,1} P_{CH_4} \sqrt{b_{2,1} P_{O_2}}}{(1 + \sqrt{b_{2,1} P_{O_2}})^2}. \tag{9}$$

Model 2. Oxygen involved in hydrocarbon formation is adsorbed in molecular form ($x = 2$)

$$R_{C_2} = \frac{k_{2,2} b_{2,2} P_{CH_4} P_{O_2}}{(1 + b_{2,2} P_{O_2})^2}. \tag{10}$$

The experimentally determined rates of hydrocarbon formation were fitted to rate equations (9) and (10) by nonlinear regression analysis. The values obtained for the rate and pseudo-adsorption constants k_2 and b_2, respectively, are listed in Table 3. The relationships $R_{C_2}(P_{O_2})$ as calculated for the two models are shown in Figs. 5 and 6. At the lowest temperature of 933 K (Fig. 5) the experimental data can be well described by model 2, whereas at the highest temperature of 1033 K (Fig. 6) model 1 is more suitable; this finding is quantified by the sums of the squared residuals of the two models at the various temperatures (see Table 8). Considering this result it is proposed that a dioxygen species is effective for hydrocarbon formation at low temperatures and an atomic oxygen species at high temperatures, respectively. This conclusion reveals parallels to results obtained by Freund *et al.* (*47*), who carried out CDA (*c*harge *d*istribution *a*nalysis) measurements over a NaOH(11 mol%)/CaO catalyst activated at reaction conditions. According to these measurements O_2^{2-} species present at temperatures below 873 K dissociate into O^- species between 873 and 1048 K.

The rate and pseudo-adsorption constants should be considered physically meaningful only in the range of applicability of the respective model.

Applicability of Different Literature-based Rate Equations

In the preceding section, mechanistic assumptions were derived from the kinetic relationships. Also since different rate equations for carbon oxide and hydrocarbon formation as well as for methane conversion have been suggested earlier, their applicability to the present data was tested. As far as a quantitative evaluation according to the pattern of relationships appeared meaningful, the data were fitted to the respective rate equations at all temperatures investigated in the present work. The sum of squared residuals between experimental and calculated values was used as a quantitative measure of the quality of data fitting and as a basis for a model discrimination by statistical means. Furthermore, the dependence of calculated and experimental rates on reactant partial pressures at 973 K is presented for illustration.

Carbon oxide formation. Rate equations for carbon oxide formation proposed earlier and included in model discrimination are listed in Table 4. According to Eq. 12 derived by Wada *et al.* (*26*) for a lanthanum boron oxide catalyst the rate of carbon oxide formation depends on the oxygen partial

TABLE 4

Kinetic Equations for Carbon Oxide Formation Reported in the Earlier Literature

Asami *et al.* (*8*)

$$R_{CO_X} = \frac{k_{10}k_{11}f_{10}(P(O_2))f_{11}(P(CH_4))}{k_{10}f_{10}(P(O_2)) + k_{11}f_{11}(P(CH_4))} \quad (11a)$$

with $f_{10}(P(O_2)) = P(O_2)$ and $f_{11}(P(CH_4)) = P(CH_4)$ (11b)

Wada *et al.* (*26*)

$$\frac{d[CO_x]}{dt} = k_6 P_O \left[\frac{k_2^{0.5}K_1^{0.5}P_M^{0.5}P_O^{0.25}}{k_3^{0.5}} - \frac{k_4}{2k_3}\right] \quad (12)$$

M is methane and O is oxygen

Iwamatsu and Aika (*27*)

$$\frac{dP_{CO_X}}{dt} = \frac{k_3^2 P_{O_2}^x}{4k_4}\left[\left[1 + \frac{8k_1k_2k_4P_{O_2}P_{CH_4}}{k_3^2P_{O_2}^x(k_1P_{O_2} + k_2P_{CH_4})}\right]^{0.5} - 1\right] \quad (13)$$

pressure with a reaction order of 1–1.25. This equation is not applicable to the present NaOH/CaO catalyst, for which the respective reaction order was observed to be 0.5. In order to check the applicability of the rate equation of Asami *et al.* (*8*, Eq. (11)), the present experimental data were fitted to this equation for all temperatures applied. The obtained sums of squared residuals are listed in Table 7. In order to check the applicability of the rate equation suggested by Iwamatsu and Aika (*27*, Eq. (13)), the following procedure was applied. The kinetic parameters k_4/k_3^2 and x of rate equation (13) (Ref. (*27*)) were determined by plotting $\ln(R_{C_2}/R_{CO_X}^2)$ against $\ln P_{O_2}$ also using rate equation (16) (Ref. (*27*)) for hydrocarbon formation (Table 5); the constants k_1 and k_2 were then obtained by fitting the total methane conversion rate to Eq. (19) (Table 6). By means of these constants the carbon oxide formation rates were calculated for the experimental methane and oxygen partial pressures according to Eq. (13) (Ref. *27*) for all temperatures applied. The sums of squared residuals are listed in Table 7. For illustration the calculated and experimental rate data at 973 K are plotted versus methane and oxygen partial pressure in Figs. 7a and 7b.

Applying the F test, the models are significantly different (level of significance, 99%) when the ratio of the variances exceeds a value of 4. Considering Figs. 7a and 7b and the sums of squared residuals in Table 7 it is evident that the kinetic equation of Asami *et al.* (*8*) and that of Iwamatsu and Aika (*27*) are capable of describing the general trend; nevertheless, the carbon oxide formation rate can be described significantly better by a power-law rate equation with a reaction order of 0.5 for both methane and oxygen.

Hydrocarbon formation. Rate equations for hydrocarbon formation proposed by various authors are listed in Table 5. Equation (14) proposed by Asami *et al.* (*8*) and Eq. (15) of Wada *et al.* (*26*) were dismissed since these equations are not capable of describing the rate maximum experimentally observed with respect to oxygen partial pressure. Rate equation (16) derived by Iwamatsu and Aika (*27*) for C_2 hydrocarbon formation was applied for all temperatures

TABLE 5

Kinetic Equations for C_2 Hydrocarbon Formation Reported in the Earlier Literature

Asami *et al.* (*8*)

$$R_{C_2} = \frac{k_3k_4f_3(P(CH_4))f_4(P(O_2))}{k_3f_3(P(CH_4)) + k_4f_4(P(O_2))} \quad (14a)$$

with $f_3(P(CH_4)) = P(CH_4)$ and $f_4(P(O_2)) = P(O_2)$ (14b)

Wada *et al.* (*26*)

$$\frac{d[C-C]}{dt} = k_2K_1P_MP_O^{0.5} - \frac{k_2^{0.5}k_4k_1^{0.5}}{k_3^{0.5}}P_M^{0.5}P_O^{0.25} \quad (15)$$

M is methane and O is oxygen

Iwamatsu and Aika (*27*)

$$\frac{dP_{C_2H_6}}{dt} = \frac{k_3^2P_{O_2}^x}{16k_4}\left[\left[1 + \frac{8k_1k_2k_4P_{O_2}P_{CH_4}}{k_3^2P_{O_2}^x(k_1P_{O_2} + k_2P_{CH_4})}\right]^{0.5} - 1\right]^2 \quad (16)$$

TABLE 6

Kinetic Equations for the Methane Conversion Reported in the Earlier Literature

Otsuka and Jinno (*6*)

$$-R_{CH_4} = k\frac{K_m P_{CH_4}}{1 + K_m P_{CH_4}}\frac{K_o P_{O_2}}{1 + K_o P_{O_2}} \quad (17)$$

Amorebieta and Colussi (*20*)

$$-R_{CH_4} = \frac{k_3 K^{1/2}[O_2]^{1/2}[CH_4]}{1 + K_1^{1/2}[O_2]^{1/2} + K_2[CH_4]} \quad (18)$$

Mars/van Krevelen-type rate law (*19, 27, 30*)

$$-R_{CH_4} = \frac{k_1 P_{O_2} k_2 P_{CH_4}}{k_1 P_{O_2} + k_2 P_{CH_4}} \quad (19)$$

Roos *et al.* (*28*)

$$-R_{CH_4} = \frac{k_r b_{O_2} P_{O_2} b_{CH_4} P_{CH_4}}{(1 + b_{CO_2} P_{CO_2})(1 + b_{CH_4} P_{CH_4} + b''_{CO_2} P_{CO_2})} \quad (20a)$$

or

$$-R_{CH_4} = \frac{k_r b_{O_2} P_{O_2} b_{CH_4} P_{CH_4}}{(1 + b_{CH_4} P_{CH_4} + b_{CO_2} P_{CO_2})^2} \quad (20b)$$

Miro *et al.* (*30*)

$$-R_{CH_4} = \frac{k_1 K P_{O_2} P_{CH_4}}{(1 + K P_{O_2})} \quad (21)$$

and partial pressures (the procedure for determining the constants k_1, k_2, k_4/k_3^2, and x has already been described above). The sums of squares of residuals are listed in Table 8. For illustration the calculated and experimental rate data at 973 K are plotted versus methane and oxygen partial pressure (see Figs. 8a and 8b). Considering these figures it is evident that Eq. (16) in Ref. (*27*) is capable of describing the general pattern (rate maximum with respect to O_2) of the relationship between the rate and the oxygen partial pressure. Nevertheless, the fit is not satisfactory, especially in the range of low partial pressures. According to the *F* test, Eqs. (9) and (10) derived by the present authors fit the experimental data in the range of their applicability significantly better than Eq. (16) in Ref. (*27*) (cf. Table 8).

Methane conversion. The various rate equations for the overall conversion of methane that have been proposed in the literature are summarized in Table 6. The equations of Roos *et al.* (*28*, Eq. 20) and Miro *et al.* (*30*, Eq. 21) can be ruled out, since for the present NaOH/CaO catalyst the methane conversion was not observed to be first order in oxygen or in methane (see Table 1). The models of Otsuka and Jinno (*6*, Eq. (17)), Amorebieta and Colussi (*20*, Eq. (18)), and the Mars/van Krevelen-type rate law (Eq. (19)) (Ref. *19, 27, 30*) were tested by fitting the experimental methane conversion rates to the respective rate equations by nonlinear regression analysis at all temperatures. The obtained sums of squares of residuals are listed in Table 9. The calculated and experimental rate data at 973 K plotted versus methane and oxygen partial pressure are shown in Figs. 9a and 9b as an illustration along with the data for the power-law rate equation (4) of this study. Considering these figures it can be concluded that the kinetic equations Eq. (17) (Ref. *6*); Eq. (18) (Ref. *20*); Eq. (19) (see above) give a satisfactory fit of the data although the power-law rate equation (4) is more suitable. According to the *F* test, Eq. (4) is significantly better than the other kinetic equations (see Table 9).

CONCLUSIONS

In the present study the effect of reactant partial pressures and temperature on the

TABLE 7

Carbon Oxide Formation: Sum of Squares of Residuals for the Respective Rate Equations

T (K)	Equation (2)	Asami *et al.* (*8*, Eq. (11))	Iwamatsu and Aika (*27*, Eq. (13))
933	7.68×10^{-13}	1.43×10^{-11}	2.84×10^{-11}
953	9.17×10^{-13}	4.42×10^{-11}	6.59×10^{-11}
973	3.08×10^{-12}	5.18×10^{-11}	6.30×10^{-11}
993	5.83×10^{-12}	8.47×10^{-11}	9.84×10^{-11}
1013	6.06×10^{-12}	1.45×10^{-10}	1.55×10^{-10}
1033	5.18×10^{-12}	2.13×10^{-10}	1.98×10^{-10}

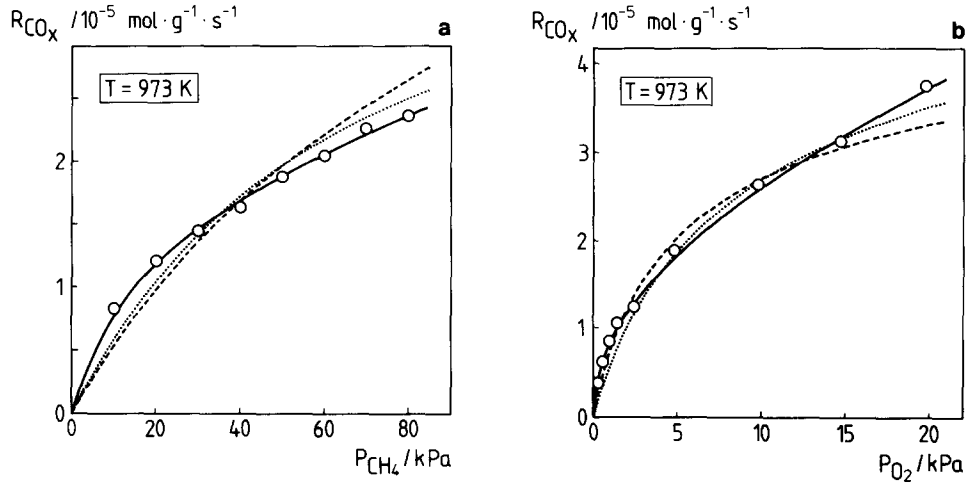

FIG. 7. Rate of carbon oxide formation versus (a) methane and (b) oxygen partial pressure at T = 973 K. Symbols, experimental data. (—) Calculated according to the power-law rate equation (2). (· · ·) Calculated according to the rate equation proposed by Asami *et al.* (*8*, Eq. (11)). (---) Calculated according to the rate equation proposed by Iwamatsu and Aika (*27*, Eq. (13)).

rate of hydrocarbon formation from methane, on its total oxidation to CO_X and on its total conversion, was investigated applying a NaOH/CaO catalyst. Furthermore, kinetic isotope effects were determined.

The carbon oxide formation is of 0.5 order both in methane and in oxygen. No kinetic isotope effect was observed for CO_X formation. Accounting for these results it was suggested that methane and oxygen reacting to CO_X adsorb dissocatively and that the rate-determining step for CO_X formation is the reaction between a CH_3 species and an O species.

The hydrocarbon formation is first order in methane and passes through a maximum with respect to oxygen partial pressure; this was suggested to be due to inhibition by adsorbed oxygen on the catalyst surface. For C_2 formation a significant kinetic isotope effect was observed; therefore the rate-determining step was assumed to be the formation of a methyl radical by C–H bond breaking. It was proposed that this reaction occurs between weakly adsorbed molecular methane and a strongly bound oxygen species.

The proposition that methane reacting to carbon oxides is adsorbed dissociatively while methane reacting to hydrocarbons is adsorbed associatively can be best explained by assuming that CO_X and C_2 are formed on different sites. This suggestion is supported by the occurrence of significantly different kinetic isotope effects for carbon oxide and hydrocarbon formation. In agreement with Nelson *et al.* (*37*) and Mirodatos *et al.* (*39*), different k_H/k_D ratios are regarded as indication that carbon oxides and hydrocarbons are formed by separate reaction pathways involving different rate-determining steps via different intermediates. Burch *et al.* (*40*) regard different active

TABLE 8

Hydrocarbon Formation: Sum of Squares of Residuals for the Respective Rate Equations

T (K)	Model 1, Eq. (9)	Model 2, Eq. (10)	Iwamatsu and Aika (27, Eq. (16))
933	2.87×10^{-13}	1.02×10^{-13}	1.67×10^{-12}
953	2.94×10^{-13}	8.95×10^{-13}	4.31×10^{-12}
973	3.31×10^{-13}	2.75×10^{-12}	4.62×10^{-12}
993	3.86×10^{-13}	9.35×10^{-12}	1.24×10^{-11}
1013	3.54×10^{-13}	2.98×10^{-11}	2.76×10^{-11}
1033	5.32×10^{-13}	1.04×10^{-10}	7.99×10^{-11}

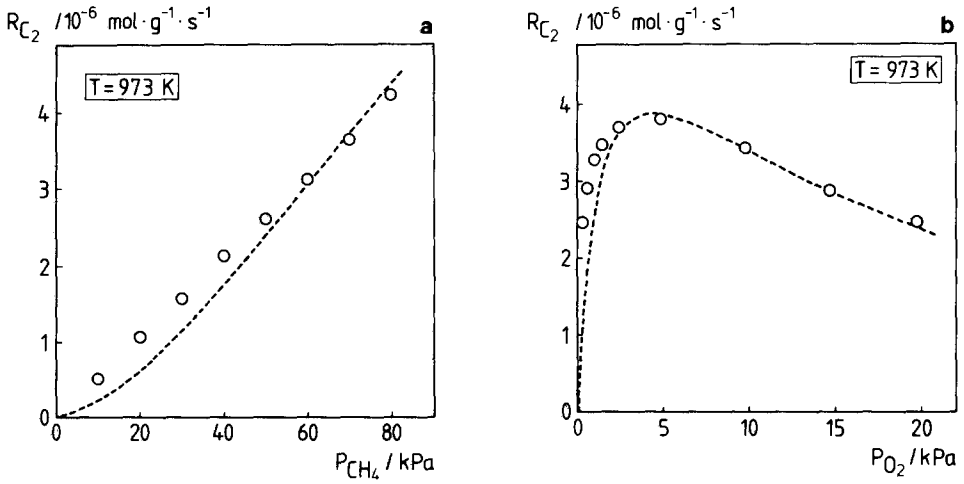

FIG. 8. Rate of hydrocarbon formation versus (a) methane and (b) oxygen partial pressure at T = 973 K. Symbols, experimental data. (---) Calculated according to the rate equation proposed by Iwamatsu and Aika (*27*, Eq. (16)).

centers for carbon oxide and hydrocarbon formation as a possible explanation for the different kinetic isotope effects observed by these authors. According to Hatano and Otsuka (*17*) and Mirodatos and Martin (*24*), significantly different pressure effects on the rates of CO_X and C_2 formation, as also observed in the present work, indicate that both reactions proceed via different reaction intermediates and on different sites. Two different types of active sites have also been proposed by other authors, for example by Sinev *et al.* (*19*) and by Hutchings *et al.* (*48*).

It was derived that a weakly adsorbed oxygen species is responsible for carbon oxide formation whereas the oxygen species effective for C_2 hydrocarbon formation is more strongly bound to the surface. Similar results have been reported by other groups. Tagawa and Imai (*11*) demonstrated by using a pulsed-flow technique that a strongly adsorbed oxygen species is effective for C_2 formation while a weakly adsorbed or gas-phase oxygen species is involved in CO_X formation over a $LaAlO_3$ catalyst. France *et al.* (*49*) considered strongly bonded oxygen to be effective for hydrocarbon formation and weakly bonded oxygen for deep oxidation over perovskite-type oxides. From pulse experiments over a Sb/SiO_2 catalyst Lo *et al.* (*16*) concluded lattice oxygen to be active for the coupling reaction, whereas adsorbed or gaseous oxygen was considered to be active for carbon oxide formation. Similar conclusions were drawn by Asami *et al.* (*8*) for a PbO/MgO catalyst and by Hatano and Otsuka (*17*) for a $LiNiO_2$ catalyst. Different oxygen species effective for CO_X and C_2 formation were also proposed by Otsuka *et al.* (*3*), by Iwamatsu and Aika (*27*), and by Spinicci (*50*).

The apparent reaction orders in methane

TABLE 9

Methane Conversion: Sum of Squares of Residuals for the Respective Rate Equations

T (K)	Equation (4)	Otsuka and Jinno (*6*, Eq. (17))	Amorebieta and Colussi (*20*, Eq. (18))	Mars/van Krevelen, Eq. (19)
933	1.27×10^{-12}	3.49×10^{-11}	9.50×10^{-11}	4.46×10^{-11}
953	1.66×10^{-12}	7.86×10^{-11}	2.43×10^{-10}	1.19×10^{-10}
973	3.96×10^{-12}	9.60×10^{-11}	6.12×10^{-11}	1.13×10^{-10}
993	5.69×10^{-12}	2.02×10^{-10}	2.09×10^{-10}	2.24×10^{-10}
1013	6.16×10^{-12}	3.66×10^{-10}	3.30×10^{-10}	4.30×10^{-10}
1033	8.52×10^{-12}	8.20×10^{-10}	1.16×10^{-10}	8.83×10^{-10}

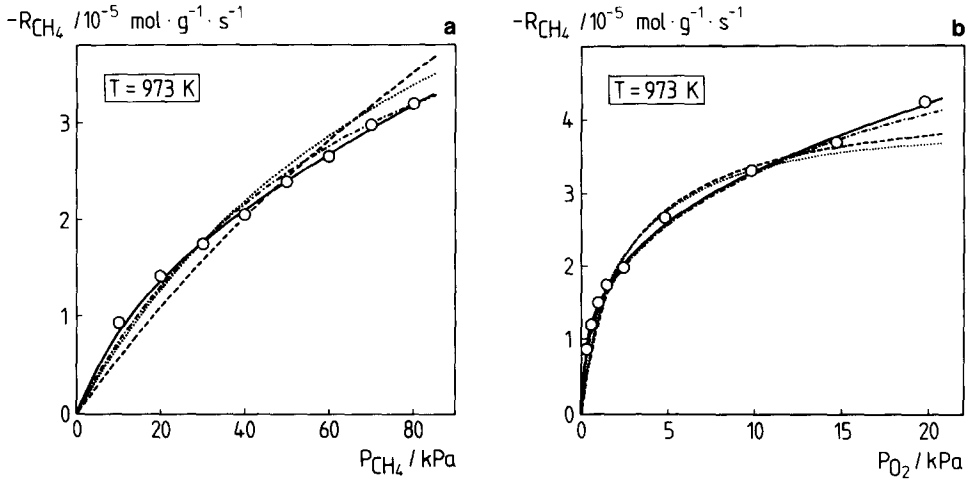

FIG. 9. Rate of methane conversion versus (a) methane and (b) oxygen partial pressure at T = 973 K. Symbols, experimental data. (—) Calculated according to the power-law rate equation (4). (· · ·) Calculated according to the rate equation proposed by Otsuka and Jinno (*6*, Eq. (17)). (- · -) Calculated according to the rate equation proposed by Amorebieta and Colussi (*20*, Eq. (18)). (- - -) Calculated according to the rate equation proposed in (*19*, *27*, *30*); Eq. (19).

and oxygen for the overall methane conversion display a dependence on temperature (see Table 1). These exponents should not be considered as physically meaningful, since a mechanistic relevance could be ascribed to the reaction orders only if both reaction paths leading to CO_X and C_2 would involve the same intermediate that was excluded because of different kinetic isotope effects.

Kinetic equations published earlier were only partly applicable to the experimental data of this study. This finding may be explained by two reasons: (1) Catalysts different from the present NaOH/CaO catalyst were applied, which may catalyze the oxidative methane coupling reaction according to a partly different mechanism, and (2) in most of the earlier studies methane and oxygen partial pressures were varied over a smaller range than that applied in this investigation.

ACKNOWLEDGMENT

This study has been supported by the Commission of the European Communities (Contract No. EN3C-0023-D).

REFERENCES

1. Hinsen, W., Bytyn, W., and Baerns, M., *in* "Proceedings, 8th International Congress on Catalysis, Berlin, 1984," Vol. III, p. 581. Dechema, Frankfurt-am-Main, 1984.
2. Ito, T., Wang, J.-X., Lin, C.-H., and Lunsford, J. H., *J. Am. Chem. Soc.* **107,** 5062 (1985).
3. Otsuka, K., Jinno, K., and Morikawa, A., *J. Catal.* **100,** 353 (1986).
4. Ali Emesh, I. T., and Amenomiya, Y., *J. Phys. Chem.* **90,** 4785 (1986).
5. Otsuka, K., and Nakajima, T., *J. Chem. Soc. Faraday Trans.* **83,** 1315 (1987).
6. Otsuka, K., and Jinno, K., *Inorg. Chim. Acta* **121,** 237 (1986).
7. Sinev, M. Y., Korchak, V. N., and Krylov, O. V., *Kinet. Katal.* **28**(6), 1376 (1987).
8. Asami, K., Shikada, T., Fujimoto, K., and Tominaga, H., *Ind. Eng. Chem. Res.* **26,** 2348 (1987).
9. Labinger, J. A., Ott, K. C., Mehta, S., Rockstead, H. K., and Zoumalan, S., *J. Chem. Soc., Chem. Commun.*, 543 (1987).
10. Labinger, J. A., and Ott, K. C., *J. Phys. Chem.* **91,** 2682 (1987).
11. Tagawa, T., and Imai, H., *J. Chem. Soc. Faraday Trans.* **84**(4), 923 (1988).
12. Keulks, G. W., and Yu, M., *React. Kinet. Catal. Lett.* **35**(1–2), 361 (1987).
13. Kimble, J. B., and Kolts, J. H., *Chemtech*, 501 (August 1987).
14. Tagawa, T., and Imai, H., *React. Kinet. Catal. Lett.* **37**(1), 115 (1988).

15. Lin, C.-H., Wang, J.-X., and Lunsford, J. H., *J. Catal.* **111,** 302 (1988).
16. Lo, M.-Y., Agarwal, S. K., and Marcelin, G., *J. Catal.* **112,** 168 (1988).
17. Hatano, M., and Otsuka, K., *J. Chem. Soc. Faraday Trans.* **85**(2), 199 (1989).
18. McCarty, J. G., Quinlan, M. A., and Sancier, K. M., Paper presented at 1988 Spring National Meeting of the American Institute of Chemical Engineers, New Orleans, Louisiana, 1988.
19. Sinev, M. Y., Korchak, V. N., and Krylov, O. V., *Kinet. Katal.* **30**(4), 855 (1989).
20. Amorebieta, V. T., and Colussi, A. J., *J. Phys. Chem.* **92,** 4576 (1988).
21. Follmer, G., Lehmann, L., and Baerns, M., *Catal. Today* **4,** 323 (1989).
22. Kooh, A., Minoun, H., and Cameron, C. J., *Catal. Today* **4,** 333 (1989).
23. Carreiro, J. A. S. P., Follmer, G., Lehmann, L., and Baerns, M., *in* "Proceedings, 9th International Congress on Catalysis, Calgary, 1988" (M. J. Phillips and M. Ternan, Eds.), Vol. II, p. 891. Chem. Institute of Canada, Ottawa, 1988.
24. Mirodatos, C., and Martin, G. A., *in* "Proceedings, 9th International Congress on Catalysis, Calgary, 1988" (M. J. Phillips and M. Ternan, Eds.), Vol. II, p. 891. Chem. Institute of Canada, Ottawa, 1988.
25. Doi, T., Utsumi, Y., and Matsuura, I., *in* "Proceedings, 9th International Congress on Catalysis, Calgary, 1988" (M. J. Phillips and M. Ternan, Eds.), Vol. II, p. 937. Chem. Institute of Canada, Ottawa, 1988.
26. Wada, S., Tagawa, T., and Imai, H., *Appl. Catal.* **47,** 277 (1989).
27. Iwamatsu, E., and Aika, K.-I., *J. Catal.* **117,** 416 (1989).
28. Roos, J. A., Korf, S. J., Veehof, R. H. J., Van Ommen, J. G. and Ross, J. R. H., *Appl. Catal.* **52,** 131 (1989).
29. Otsuka, K., Murakami, Y., Wada, Y., Said, A. A., and Morikawa, A., *J. Catal.* **121,** 122 (1990).
30. Miro, E. E., Santamaria, J. M., and Wolf, E. E., *J. Catal.* **124,** 465 (1990).
31. Burch, R., Tsang, S. C., and Swarnakar, R., *J. Chem. Soc. Faraday Trans.* **86**(22), 3803 (1990).
32. Ding, X., Yu, Z., Wang, X., and Shen, S., *Stud. Surf. Sci. Catal.* **61,** 65 (1991).
33. Bartsch, S., Pirkl, H.-G., Baumann, W., and Hofmann, H., *Stud. Surf. Sci. Catal.* **61,** 147 (1991).
34. Lehmann, L., and Baerns, M., *Cat. Today,* in press.
35. Seel, O., and Baerns, M., unpublished results.
36. Campbell, K. D., and Lunsford, J. H., *J. Phys. Chem.* **92,** 5792 (1988).
37. Nelson, P. F., Lukey, C. A., and Cant, N. W., *J. Catal.* **120,** 216 (1989).
38. Keulks, G. W., and Yu, M., "Preprints for New Developments in Selective Oxidation," Paper G.6. Univ. Bologna, Italy 1989.
39. Mirodatos, G., Holmen, A., Mariscal, R., and Martin, G. A., *Catal. Today* **6,** 601 (1990).
40. Burch, R., Tsang, S. C., Mirodatos, C., and Sanchez M., J. G., *Catal. Lett.* **7,** 423 (1990).
41. Slagle, I. R., and Gutman, D., *J. Am.Chem. Soc.* **107,** 5342 (1985).
42. Zanthoff, H., Ph.D. thesis, Ruhr-University Bochum, Germany, 1991.
43. Lunsford, J. H., *Stud. Surf. Sci. Catal.* **61,** 3 (1991).
44. Mims, C. A., Hall, R. B., Rose, K. D., and Myers, G. R., *Catal. Lett.* **2,** 361 (1989).
45. Otsuka, K., Inaida, M., Wada, Y., Komatsu, T., and Morikawa, A., *Chem. Lett.,* 1531 (1989).
46. Cant, N. W., Lukey, C. A., Nelson, P. F., and Tyler, R. J., *J. Chem. Soc., Chem. Commun.,* 766 (1988).
47. Freund, F., Maiti, G. C., Batllo, F., and Baerns, M., *J. Chim. Phys.* **87**(7–8), 1467 (1990).
48. Hutchings, G. J., Scurrell, M. S., and Woodhouse, J. R., *J. Chem. Soc., Chem. Commun.,* 765 (1989).
49. France, J. E., Shamsi, A., and Ahsan, M. Q., *Energy Fuels* **2,** 235 (1988).
50. Spinicci, R., *Stud. Surf. Sci. Catal.* **61,** 173 (1991).